

Maricel Alvarez · Armin Gieseke ·
Roberto Godoy · Steffen Härtel

Surface-bound phosphatase activity in ectomycorrhizal fungi: a comparative study between a colorimetric and a microscope-based method

Received: 6 June 2005 / Revised: 16 September 2005 / Accepted: 20 September 2005
© Springer-Verlag 2005

Abstract For the quantification of surface-bound phosphomonoesterase activity (SBPA) of fungi, roots, or mycorrhiza, a colorimetric method based on *p*-nitrophenyl phosphate (pNPP) is widely used. Unfortunately, this method does not reveal information about the localization of the surface-bound phosphomonoesterase (SBP). We introduce a method that localizes and quantifies SBPA in living hyphae of ectomycorrhizal fungi using confocal laser scanning microscopy of the hydrophilic substrate enzyme-labelled fluorescence (ELF-97) and compare it to the pNPP assay. ELF-97 turns into a strongly fluorescent precipitate upon activation by SBPA and forms bright fluorescent centres on the outer cell wall of the hyphae. Our data show that the enzymatic reaction is not substrate-limited during an incubation period of 15 min in fungal hyphae of *Pisolithus tinctorius*, *Cenococcum geophilum*, and *Paxillus involutus*. Image-processing routines determined the total intensity and the average number of the fluorescent ELF-97 centres per micrometre fungal hyphae of *C. geophilum* and *Paxillus involutus*. ELF-97 and pNPP detected similar variations of the SBPA at different pH values (3–7) during the measurement and different phosphorus (P) concentrations during the growth period of the fungi. The ELF-97 method revealed that *C. geophilum* and *Paxillus involutus* adapt in different ways to the variation of the P concentrations during the growth period by

varying the number, the activity, or both properties of the SBP centres. The phosphatases show peak activities at different pH values, so the response of the fungal mycelium to varying P concentrations in soils is pH selective. In conclusion, ELF-97 is a promising substrate to reveal SBPA and adaptation strategies on a structural–physiological level.

Keywords Surface-bound phosphatase activity · ELF-97 · *p*-Nitrophenyl phosphate · Image processing · Quantitative fluorescence microscopy

Introduction

The phosphatase activity of mycorrhiza, extramatrix mycelia, and roots is of vital importance for the supply of plants with phosphorus (P) (Joner and Johansen 1999). Phosphomonoesterases and phosphodiesterases mineralize the organic P reservoirs in soils and convert it into a plant-accessible nutrient (Smith and Read 1997). The P-cleaving enzymes are commonly separated into an intracellular fraction, a surface-bound or cell-wall-associated fraction, and an extracellular fraction, which can be isolated from sample tissue by filtration (McElhinney and Mitchell 1993). The most frequently used technique for the determination of phosphatase activities is based on the hydrolysis of *p*-nitrophenyl phosphate (pNPP) to *p*-nitrophenol phosphate (pNP) + P (see review by Tibbett 2002). This colorimetric method is reported to work reliably when it comes to the determination of the extracellular and the intracellular enzyme fraction (McElhinney and Mitchell 1993). However, when it comes to the determination of the surface-bound phosphomonoesterase activity (SBPA) in mycelium or roots, several drawbacks of the colorimetric assay have been outlined (Tibbett et al. 2000; Tibbett 2002). The most important drawback of the colorimetric assay is that no structural information about the surface-bound phosphomonoesterase (SBP) centres on the sample surfaces is obtained. Methods that access such features are based either on bright field microscopy in combination with Fast Blue RR-salt (Tisserant et al. 1993) or on fluorescence micros-

M. Alvarez (✉) · R. Godoy
Instituto de Botánica, Universidad Austral de Chile,
Campus Isla Teja, Casilla 567,
Valdivia, Chile
e-mail: malvarez@uni-bremen.de
Tel.: +56-63-293490
Fax: +56-63-221313

A. Gieseke
Max Planck Institute for Marine Microbiology,
Bremen, Germany

S. Härtel
Centro de Estudios Científicos (CECS),
Arturo Prat 514,
Valdivia, Chile

copy using the enzymatic activation of the fluorogenic substrate enzyme-labelled fluorescence (ELF-97; van Aarle et al. 2001; Alvarez et al. 2004, 2005).

In this work, we show that the enzymatic activation of the fluorogenic substrate ELF-97 reveals qualitative and quantitative information of the SBPA in mycelium of ectomycorrhizal (EM) fungi. Our technique combines quantitative measurements of the fluorescence intensities by confocal laser scanning microscopy (LSM) with the localization of SBPA on the fungal hyphae by subsequent image-processing routines. We follow the reaction kinetics of the ELF-97 activation in mycelium of *Pisolithus tinctorius*, *C. geophilum*, and *Paxillus involutus* and determine SBPA in mycelium of *C. geophilum* and *Paxillus involutus* under the variation of the pH values during the measurements and under the variation of the P supply during the growth period of the fungi. The quantitative results of the microscopic method are compared directly to the colorimetric method based on pNPP. Finally, we discuss the applicability of our method for the determination of SBPA in EM associations and in roots from experimental areas.

Materials and methods

Cultivation of fungi

Cultures of the EM fungi *Paxillus involutus* (Batsch: Fr.) Sing. were obtained from fruiting bodies that were collected in temperate forests of *Nothofagus obliqua* (Mirb.) Oerst., located near Quita Calzón, 39°78'S, 73°02'W, Valdivia, X Region, Chile. Ectomycorrhizae of *C. geophilum* Fr. were also collected at this site, but the fungi were isolated from EM mantle sections. *Pisolithus tinctorius* (Pers.) Coker & Couch (isolate 441) was obtained from cultures maintained at the Institute of Environmental Science and Technology, University of Bremen, Germany. Inoculum plugs of $\varnothing=7$ mm were transferred from solid Melin–Norkrans culture media [malt extract 5 g/l, D-glucose 10 g/l, $(\text{NH}_4)_2\text{HPO}_4$ 0.25 g/l, KH_2PO_4 0.5 g/l, $\text{MgSO}_4 \cdot 7\text{H}_2\text{O}$ 0.15 g/l, CaCl_2 0.05 g/l, Fe–EDTA 0.022 g/l, NaCl_2 0.025 g/l, thiamine HCl 1×10^{-4} g/l; Molina and Palmer 1982] to 50 ml of liquid culture media in culture flasks. Fungi were cultivated in the dark at 25°C and pH 5 with 0, 1.7, 3.4, and 5.6 mM of dissolved phosphate (5.6 mM = 0.5 KH_2PO_4 g/l + 0.25 $(\text{NH}_4)_2\text{HPO}_4$ g/l) in the liquid culture media. A cultivation period of 2 weeks was determined as described earlier (Straker and Mitchell 1986). After 2 weeks, fungi were harvested, and SBPA was determined by both a colorimetric method and an alternative method based on quantitative fluorescent microscopy as described below.

Colorimetric quantification of SBPA

Surface-bound phosphomonoesterase activity of all EM fungi was determined by a colorimetric standard method based on pNPP (Merck 1.06850.0025, Germany) according

to Tibbett et al. (1998). Buffer solutions containing Tris (hydroxymethyl)aminomethane (3.025 g/l), maleic acid (2.9 g/l), citric acid (3.5 g/l), boric acid (1.57 g/l), and 1 M NaOH (122 ml/l) were adjusted to pH 3–7 by 1 M HCl. SBP hydrolysed pNPP to pNP + P that induced a shift in the absorption wavelength from 315 to 407 nm. Five independent experiments were realized for each pH and P condition.

Fluorescence imaging by LSM

Fluorescence imaging was performed by LSM (LSM 510, ZEISS, Göttingen, Germany), equipped with a 364-nm wavelength UV–argon ion laser (Enterprise II-653, Coherent, Santa Clara, CA, USA). Fungal mycelium was stained with the hydrophilic, weakly fluorescent ELF-97 substrate, which is converted into a highly fluorescent hydrophobic precipitate upon enzymatic cleavage of the phosphate residuum (Fig. 1a). After the staining procedure (see below), two-channel picture series were recorded ($63\times$ objective, intensity $I(x,y) \in [0, 255]$, $x/y \in [0, 511]$ pixels). In channel 1 (green colour table), autofluorescence of fungal mycelium was visualized by a 385- to 470-nm band-pass filter. Channel 2 (green colour table) received light through a 560- to 615-nm band-pass filter, monitoring the fluorescence intensities of the enzymatically activated ELF-97 that precipitated around the SBP centres of the hyphae (Fig. 1).

Preparation of ELF-97 staining solutions at different pH

Buffer solutions were adjusted to pH 3, 4, 5, 6, and 7 with 1 M HCl. Fluorescent ELF-97 substrate solution was prepared by mixing ELF-97 stock solution (E-6588, Molecular Probes, Europe b.v., Leiden, The Netherlands; 5 mM in sterile water) with the corresponding buffer solutions (10:2 v/v, buffer/ELF-97 stock solution). The pH was controlled after preparation in the microvolumes of the ELF-97 substrate solution via direct measurements with pH microelectrodes. The shielded liquid-ion exchange-type pH microelectrodes had a tip diameter of 5 μm and were prepared as described earlier (de Beer et al. 1997). A three-point calibration was performed with commercial standard buffer solutions of different pH.

Determination of fluorescence kinetics of ELF-97 activation

Mycelium was removed from culture medium with tweezers and rinsed with buffer solution (pH 5). Young mycelium ($\varnothing \sim 2$ mm, ~ 5 mm thick) was separated from the outer part of the growing disc with scalpels and was transferred to microscopic cover slides. After the addition of 5 μl ELF-97 phosphatase substrate solution (pH 5), slides were covered by small plastic taps to avoid evaporation and were subjected immediately to confocal

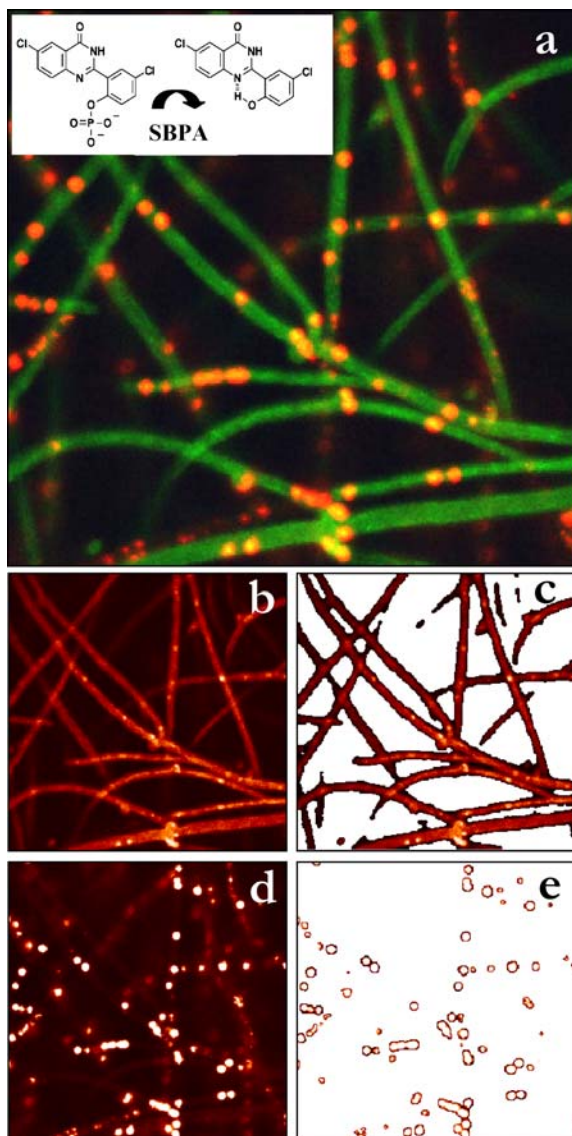


Fig. 1 Segmentation of fungal hyphae and of fluorescent enzyme-labelled fluorescence (ELF-97) centres of *Pisolithus tinctorius*. **a** Representative two-channel laser scanning microscopy (LSM) image of in vivo stained fungal hyphae (excitation at 364 nm). Channel 1, 385- to 470-nm band-pass filter detects autofluorescence of fungal mycelium (green). Channel 2, 560- to 615-nm band-pass filter detects enzymatically activated ELF-97 fluorescence intensity (red). The presented two-channel image merges the green and the red colour table of the individual images and produces a yellow colour where both subjacent fluorescence intensities are high. The inset shows the conversion of the hydrophilic, weakly fluorescent ELF-97 substrate (left) to the enzymatically activated, highly fluorescent hydrophobic ELF-97 precipitate (right) by surface-bound phosphomonoesterase activity (SBPA). **b** Autofluorescence of fungal mycelium (channel 1). **c** Result of segmented fungal mycelium. **d** Enzymatically activated fluorescent ELF-97 centres (channel 2). **e** Result of segmented ELF-97 centres

microscopy. Regions of interest were defined around the enzymatically activated ELF-97 centres (Fig. 1) by the ZEISS imaging software. Fluorescence was monitored every 3 min until the intensities reached a plateau (Fig. 2a). Subsequently, additional 5 μ l of ELF-97 phosphatase substrate solution was added to the reaction volume, and the

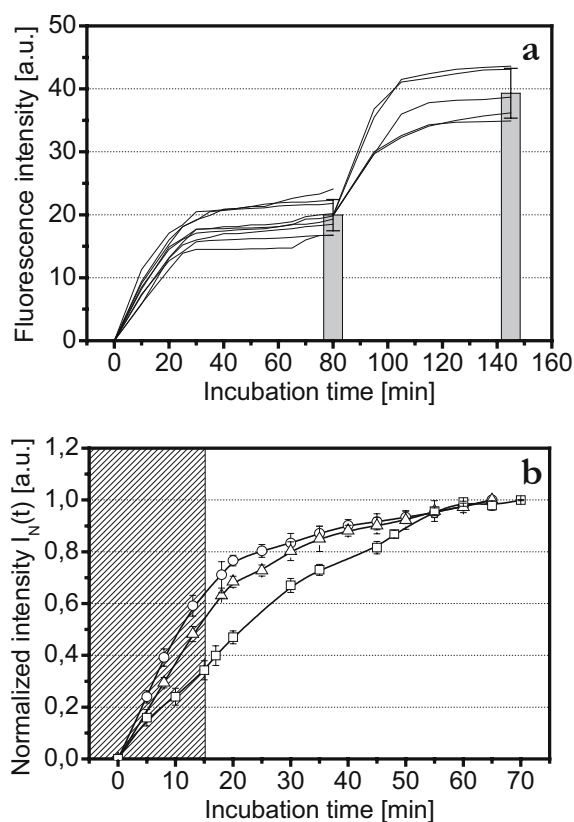


Fig. 2 Fluorescence kinetics of ELF-97 activation on fungal hyphae of *Pisolithus tinctorius*, *Paxillus involutus*, and *C. geophilum*. **a** Fluorescence intensities of activated ELF-97 precipitate in fungal hyphae of *Pisolithus tinctorius*. ELF-97 substrate was added at $t=0$ and $t=80$ min. During the first incubation cycle ($t=0-80$ min), fluorescence intensities $I(t)$ of individual ELF-97 precipitate centres on fungal hyphae were determined and scaled to the same initial value by $I(t)=I(t)-I(t=0)$. The same procedure was repeated during the second incubation cycle ($t=80-150$ min) where fluorescence intensities were scaled to an initial intensity value of $I=20$ (mean intensity value of all SBPA centres after the first incubation cycle) by $I(t)=I(t)-I(t=80)+20$. Columns show mean values and standard deviation after the first ($t=80$ min) and after the second incubation cycle ($t=140$ min). **b** Normalized fluorescence kinetics of ELF-97 activation in fungal hyphae of *Pisolithus tinctorius* (circles), *Paxillus involutus* (triangles), and *C. geophilum* (squares). For each fungus, the time-dependent fluorescence intensities $I(t)$ of five to ten phosphatase-active centres were determined and normalized by $I_N(t)=[I(t)-I(t=0)]/[I(t=70)-I(t=0)]$. Mean values and standard deviations were calculated from these normalized intensities $I_N(t)$. Striped region marks the period of linear increase of fluorescence intensities of ELF-97 centres

procedure was repeated as before. Five independent experiments yielded equivalent kinetics. Figure 2a shows the data of several SBP centres in one representative experiment.

Preparation and staining of mycelium with ELF-97 at different pH (3–7)

Pieces of mycelium were prepared as described before. Five microlitres of ELF-97 phosphatase substrate solution of the corresponding pH (3–7) was added to 100- μ l

microcentrifuge tubes containing mycelium. After an incubation of 15 min, mycelium was removed from the ELF-97 solution with tweezers and was rinsed with buffer solution at the corresponding pH (3–7) to remove all uncleaved ELF-97 substrate. Mycelium was transferred to a small depression, ground into the surface of microscopic object slides (radius 1.5–2 mm, depth ~0.5 mm), and buffer solution (pH 3–7) was added to fill out the notch. Samples were covered with microscopic cover slides, and edges were sealed with nail polish.

In vivo localization and quantification of SBPA by image-processed quantitative fluorescence microscopy

Image-processing routines for the segmentation of structures and the quantification of different parameters were programmed in Interactive Data Language (Research Systems, Co., USA). Segmentation of fungal mycelium (channel 1) and of individual fluorescent ELF-97 precipitate centres (channel 2) was achieved by interactive selection of threshold values in the intensity histograms of the corresponding images (Fig. 1). Both segmentations were completed by a successive treatment with opening/closing operators (Härtel et al. 2003, 2005a,b). From the segmented fungal hyphae and fluorescent ELF-97 centres, we calculated (1) the total intensity (I) of the fluorescent ELF-97 centres per micrometre fungal hyphae ($I \cdot \mu\text{m}^{-1}$) and (2) the average number (N) of fluorescent ELF-97 centres per micrometre fungal hyphae ($N \cdot \mu\text{m}^{-1}$). For the calculation of the hyphal length in each image, we divided the total surface area of the segmented hyphae (Fig. 1b,c) by the mean diameter of the respective type of fungal hyphae. The mean diameter was previously calculated with the ZEISS LSM 510 software from 30 hyphal diameters (Fig. 1b). A similar procedure has been applied by Antibus et al. (1997) for the estimation of the total length of collected roots. Finally, the total number of SBP centres (Fig. 1d,e) was divided by the hyphal length in each image. For three independent experiments, ten two-channel images were analysed for each experiment. Mean values were derived and plotted in Fig. 4.

Results

Saturation kinetics of enzymatically activated ELF-97 and control of pH value

Figure 2a shows the time-dependent increase in the fluorescence intensities of individual centres of enzymatically activated ELF-97 precipitate on fungal mycelium of *Pisolithus tinctorius* during two consecutive incubation cycles with the ELF-97 substrate solution (line graphs). For both incubation cycles, the fluorescence activation kinetics of ELF-97 followed the trajectory of a substrate-limited enzymatic reaction. During the first part of the reaction (~0–20 min, Fig. 2), fluorescence intensities increased

linearly to the amount of fluorescence-activated ELF-97. When the ELF-97 substrate became limited (~20–40 min, Fig. 2), a saturation of the fluorescence intensity values could be observed until the reaction finally stopped. After the second incubation cycle, the mean fluorescence of the ELF-97 centres doubled its intensities with respect to the first incubation cycle (see columns in Fig. 2a). This substrate-limited fluorescence activation kinetics of ELF-97 and its behaviour was not only observed for *Pisolithus tinctorius*, but also for *Paxillus involutus* and *C. geophilum* (Fig. 2b). By considering the fluorescence activation kinetics, an incubation period of 15 min was chosen for all subsequent microscopic measurements because this time interval assures that the fluorescence was measured within the linear range of the reaction.

To control that pH values had no effect on the fluorescence intensities of the ELF-97 precipitate, the mycelia of *Pisolithus tinctorius*, *Paxillus involutus*, and *C. geophilum* were subjected to different pH values (3–7) after the saturation of the fluorescence intensities of SBP centres had been reached. The intensity of ELF-97 precipitate centres remained stable by changing the pH value (results not shown). Additionally, we checked whether the pH value (3–7) remained constant during the 2-h incubation period of *Pisolithus tinctorius*, *Paxillus involutus*, or *C. geophilum* with the ELF-97 substrate solution. No significant changes were registered in the first 15 min, whereas the pH values increased within 2 h by less than 7% for pH values in the range of 4–7 and almost by 40% at pH 3 (data not shown).

Determination of SBPA by pNPP assay

The results of the colorimetric determination of SBPA in the mycelium of *C. geophilum* and *Paxillus involutus* are presented in Fig. 3. The SBPA showed a strong variability with P concentration and pH values. The SBPA of *C. geophilum* showed a maximum value of $12 \mu\text{mol [pNP] g}^{-1} \text{ h}^{-1}$ at pH 5 and at a P concentration of 3.4 mM. The highest SBPA value of *Paxillus involutus* was $110 \mu\text{mol [pNP] g}^{-1} \text{ h}^{-1}$ at pH 4.5 and at P concentrations of 1.7 and 3.4 mM. Both fungi showed minimum SBPA values at pH values of 3 and 7.

Comparison of microscopic and colorimetric methods for the determination of SBPA

A direct comparison of the colorimetric and the microscopic methods for the determination of SBPA in mycelium of *C. geophilum* and *Paxillus involutus* is shown in Fig. 4. SBPA values are represented by bivariate grey-scale-coded histograms in dependence of the P concentration during the growth period (x -axis) and of the pH value during the measurements (y -axis). As can be observed in Fig. 4a–d, the colorimetric and the microscopic methods produced similar results. A single SBPA maximum was determined at pH 5 and at P concentrations of 3.4 mM for *C.*

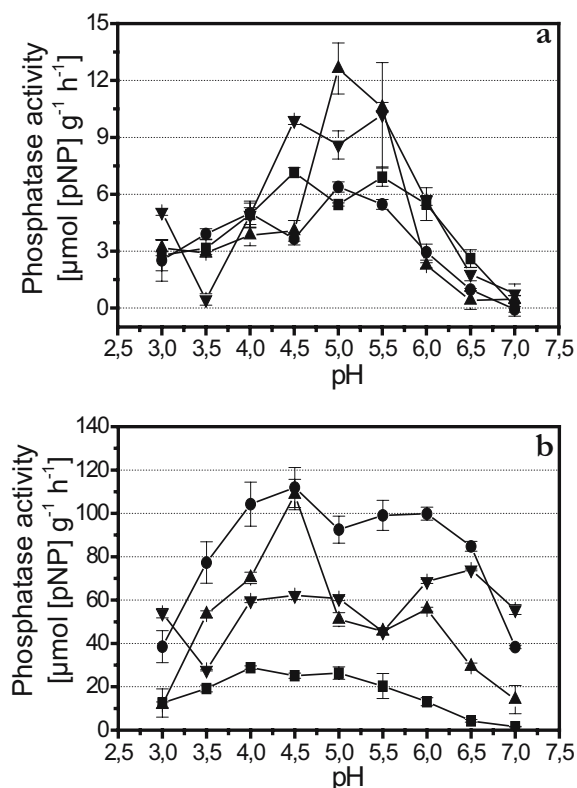


Fig. 3 Changes in SBPA of fungal hyphae of *C. geophilum* (a) and *Paxillus involutus* (b) as determined by a colorimetric method based on *p*-nitrophenyl phosphate (pNPP) in response to pH. Fungal hyphae were cultured at different P concentrations (in mM): 0 (squares), 1.7 (circles), 3.4 (up-triangle), and 5.6 (down-triangle). Mean values and standard deviations are plotted for five independent experiments

geophilum. Two peaks of enzyme activity were detected at P concentrations of 1.7 mM and pH values of 4 and 6 for *Paxillus involutus*. Only marginal differences between the methods can be observed. For the mycelium of *Paxillus involutus*, the SBPA peaks determined with ELF-97 (Fig. 4d) are more pronounced than the ones determined with the pNPP method (Fig. 4b). For the mycelium of *C. geophilum*, the SBPA peak at pH 5 in response to P concentration determined with the pNPP method (Fig. 4a) is broader than the peak determined with ELF-97 (Fig. 4c). Additionally, a small SBPA enhancement can be observed at pH 3–4 at a P concentration of 0 mM, which was not reflected by the pNPP method (Fig. 4a).

Apart from the quantitative determination of the SBPA [fluorescence intensity/hyphal length ($I \cdot \mu\text{m}^{-1}$); Fig. 4c,d], structural information was derived with the microscopic method by counting the number of SBP centres/hyphal length ($N \cdot \mu\text{m}^{-1}$; Fig. 4e,f) for the mycelium of *C. geophilum* and *Paxillus involutus*. For *C. geophilum* (Fig. 4c,e), the distribution of the quantitative parameters and of the structural parameters in dependence of the pH values and the P concentration were very similar. On the other hand, the distribution of the quantitative parameters (Fig. 4d) for *Paxillus involutus* was different from the distribution of the structural parameters (Fig. 4f). Variations in the structural organization of the SBP centres on

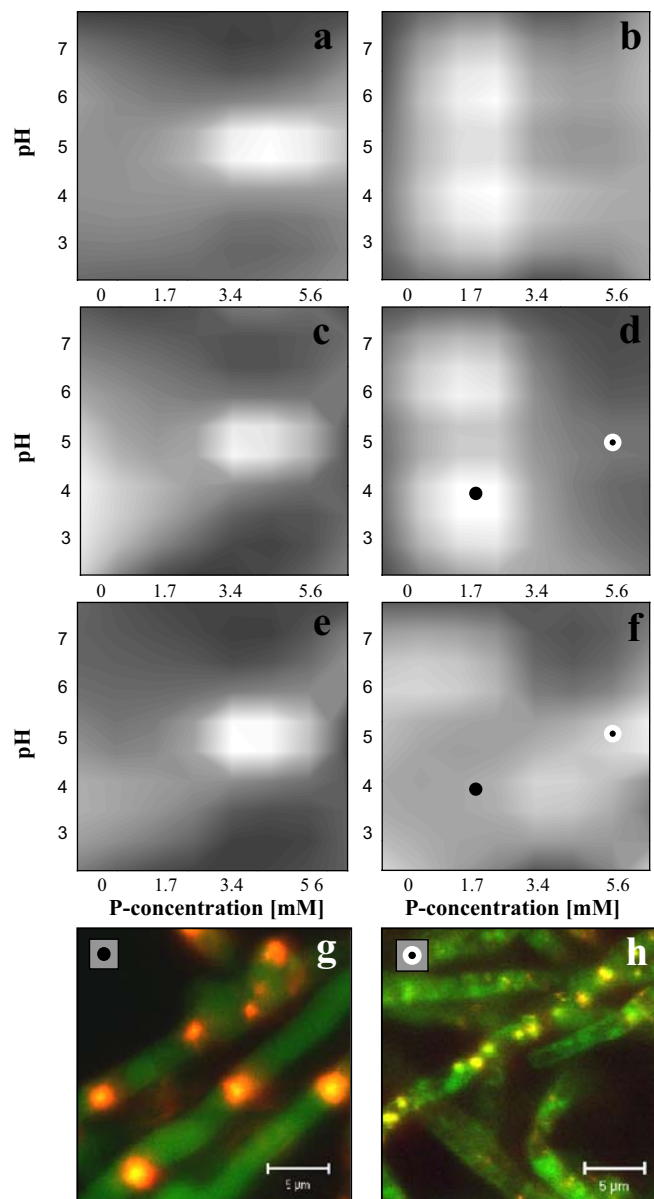


Fig. 4 SBPA of fungal hyphae of *C. geophilum* and of *Paxillus involutus* as determined by pNPP and by image-processed LSM based on fluorescence activation of ELF-97 substrate. **a, b** Bivariate grey-scale-coded presentation of SBPA of *C. geophilum* (a) and of *Paxillus involutus* (b) as determined by pNPP. **c, d** Bivariate grey-scale-coded presentation of SBPA of *C. geophilum* (c) and of *Paxillus involutus* (d) as determined by image-processed LSM. **e, f** Bivariate grey-scale-coded presentation of the number of fluorescent centres of precipitated ELF-97 substrate per micrometre hyphal length of *C. geophilum* (e) and of *Paxillus involutus* (f) as determined by image-processed LSM. For **a–f**, mean values were derived from three independent experiments. The bivariate plots (**a–f**) were successively coded by 50 intervals between *black* (minima) and *white* (maxima). **g, h** Representative fluorescence images of hyphae of *Paxillus involutus* at pH 4 and P = 1.7 mM (**g**), and at pH 5 and P = 5.6 mM (**h**). As in Fig. 1, the two-channel images merge the *green* and the *red* colour table of the channels, which produces a *yellow* colour where both subjacent fluorescence intensities are high

the hyphae of *Paxillus involutus* can be observed in Fig. 4g and h (the corresponding pH and the P conditions are marked in Fig. 4d,f).

Discussion

More than a decade ago, Kamentsky and Kamentsky (1991) reported that microscopes can quantify fluorescence intensities. Since then, many different applications taking advantage of quantitative fluorescence microscopy have emerged (for an overview, see Darzynkiewicz et al. 2001). With respect to soil micro-organisms, different applications have recently been reviewed by Li et al. (2004) who emphasized the importance of microscopic methods to reveal structural information to soil ecological studies.

The conditions of the enzymatic reaction in situ have to be controlled carefully when substrate-dependent enzymatic reactions are determined with fluorescence microscopy. Our results concerning the saturation kinetics of the enzymatically activated substrate ELF-97 (Fig. 2) and the pH stability during and after the incubation period demonstrate the following: (1) the enzymatic reaction during an incubation period of 15 min is not substrate-limited (Fig. 2); (2) the pH values (3–7) remain unaltered during this period; (3) the pH value does not interfere with the quantum yield of the activated ELF-97 fluorophore; and (4) the fluorescence of the precipitated ELF-97 centres is very stable in time. Our results agree with van Aarle et al. (2001) who reported that precipitated ELF-97 centres were not dissolved at pH values below 8.5.

While prerequisites (1–4) are essential for a reliable determination of enzymatic activities by quantitative fluorescence microscopy, the following questions emerge from the observed distribution of the fluorescence pattern on the fungal hyphae (Fig. 1):

- Where are the phosphatase active sites located on the hyphae?
- Where does the fluorescence-activated, hydrophobic ELF-97 precipitate?

SBP centres were detected on the cell wall of EM fungi by electron microscopy (Dexheimer et al. 1986). Van Aarle et al. (2001) obtained identical results with a staining method based on ELF-97 and a microscopic bright-field method based on Fast Blue RR-salt (Tisserant et al. 1993) to microscopically detect SBP centres on fungal hyphae of saprophytic and vesicular–arbuscular mycorrhiza. Their observations confirm the location of ELF-97 precipitate on the periphery of the EM hyphae shown in Figs. 1 and 4g,h. However, van Aarle et al. (2001) reported some residual fluorescent ELF-97 conglomerate inside the vacuoles of the hyphae, although the hydrophobic environment of the hyphal membranes should present an efficient barrier for the strongly hydrophilic ELF-97. In EM hyphae of *Pisolithus tinctorius*, *C. geophilum*, and *Paxillus involutus*, ELF-97 fluorescence was detected exclusively on the cell wall. This observation also holds for *Austropaxillus boletinoides* (Sing.) Brsky & Jarosh and *Descolea antarctica*

(Alvarez et al. 2004). Based on determinations with pNPP, McElhinney and Mitchell (1993) detected less than 4% of the total phosphatase activity in the cytoplasm of four isolated EM fungi. In this context, van Aarle et al. (2001) remarked that LSM should be applied to get a better definition of the precipitated ELF-97 centres.

We considered two possible models for the formation of the observed fluorescent spots on the cell wall. (1) Phosphatases are organized in centres on the cellular membrane or the cell wall. The hydrophilic ELF-97 is cleaved by phosphatases to the hydrophobic ELF-97, which immediately crystallizes near these sites. (2) Phosphatases are homogeneously distributed over the cellular membrane or the cell wall, and the crystallization of cleaved ELF-97 molecules may occur in defined hydrophobic centres, e.g., hydrophobins (Wessels 1994). Both models agree with the fluorescence kinetics observed during the first and the second incubation cycle (Fig. 2a) and all the other experiments. Although a homogeneous distribution of phosphatases on the cell wall provides a greater contact surface for available substrate with possible advantages for the assimilation of nutrients, we favour the first model (see below).

The comparative determination of SBPA with ELF-97 and pNPP in mycelium of *C. geophilum* and *Paxillus involutus* yielded very similar pattern in response to changes in pH values and P concentration during the incubation period (Fig. 4a–d). The remaining differences could be explained by a series of intrinsic difficulties of the pNPP method used to determine SBPA as summarized by Tibbett (2002). Within the investigated pH range (3–7), the colorimetric method detected similar results for the amount of SBPA in mycelium of *C. geophilum* as published by Antibus et al. (1986, 1992) who determined optimum pH values between 4.5 and 5, in three out of four isolates of *C. geophilum*. SBPAs depend on soil conditions such as pH and temperature, or on the concentration of plant available P (Antibus et al. 1986, 1992). While many authors report an inverse correlation of SBPA with the P concentration in soil (Alexander and Hardy 1981; Nannipieri et al. 1990; Tibbett et al. 1998), other authors report the opposite (Straker and Mitchell 1986; McElhinney and Mitchell 1993) or no correlation at all (Dighton 1983). In *C. geophilum* and *Paxillus involutus*, a correlation between SBPA and P concentration during the growth period of the fungi could not be confirmed. In contrast to the SBPA, the extracellular fraction of phosphate-cleaving enzymes is not controlled by the available P (Nannipieri et al. 1990).

The direct comparison of the integral SBPA per micrometre hyphal length ($I \cdot \mu\text{m}^{-1}$, Fig. 4c,d) with the number of fluorescent centres per micrometre hyphal length ($N \cdot \mu\text{m}^{-1}$, Fig. 4e,f) shows that changes in the total SBPA for *C. geophilum* were primarily due to changes in the number of fluorescent centres located on the hyphal surface. For *Paxillus involutus*, different patterns were detected for both variables (Fig. 4d,f). As can be observed in Fig. 4g and h, the number of the SBP centres changes independently of the intensity. While the SBPA peak at pH 4 and at a P concentration of 1.7 mM (Fig. 4d,f,g) is due to very few SBP centres with a high intrinsic fluorescence intensity (Fig. 4g),

a higher number of SBP centres exist at pH 5 and at a P concentration of 5.6 mM (Fig. 4d,f,h), which provide rather low intrinsic activities (Fig. 4h). This observation supports our hypothesis that hydrophobic ELF-97 molecules crystallize immediately near phosphatase active sites since it seems unlikely that the structure of hydrophobic centres is altered by the variation of the applied parameters. In consequence, our data demonstrate that *C. geophilum* and *Paxillus involutus* respond in different ways to the variation of growth conditions (P concentrations and pH values). As reported earlier (Straker and Mitchell 1986), a growth period of 14 days is sufficient for the adaptation of cultured fungi to different P concentrations. In contrast, the fungi do not adapt to varying pH conditions during the short incubation period (15 min for ELF-97/1–2 h for pNPP). Our data suggest that *C. geophilum* and *Paxillus involutus* respond to growth conditions at different P concentrations by varying the number, the activity, or both properties of the SBP centres. The expressed phosphatases possess optimum activities at different pH values, so the response of the fungal mycelium to varying P concentrations in soils shows to be pH selective.

In conclusion, the microscopic technique based on ELF-97 leads to a precise anatomical and physiological description of SBPA in mycelium of EM fungi *in vivo* and allows the comparative determination of quantitative and qualitative parameters. It must be outlined that our method is not yet calibrated and can only detect relative differences of ELF-97 fluorescence of the centres. With respect to the qualitative determination with ELF-97 ($N \cdot \mu\text{m}^{-1}$), N represents the fluorescent spots in the confocal volume of the microscope, which is defined by the point spread function. Fluorescent spots, which are shielded by the hyphae, are not detected. Since the distribution of the ELF-97 centres on the surface of the fungal hyphae is isotropic, the shielded centres represent a defined fraction of the detected centres. Their number could easily be estimated based on the size of the fluorescent ELF-97 centres and the hyphal diameter. Generally, our method opens the access for the evaluation of further quantitative-morphological parameters from the segmented regions. Size distribution and fluorescence densities of SBP centres are only two possible parameters, and they may play an important role when the method will be expanded for future applications. The method also allows to include more complex anatomical criteria such as mantle organization (Alvarez et al. 2005), rhizomorphs (Schweiger et al. 2002), or arbuscules (Dickson and Kolesik 1999). In the future, this method should be applied to root material that is directly extracted from its natural habitat to gain further insight into the strategies of enzyme-driven P solubilization *in situ*.

Acknowledgements Maricel Alvarez is a postdoctoral fellow of Mecesup UCO 02–14 (Chile). This study is a contribution to Fondecyt 1040913 (Chile). Steffen Härtel is supported by Fondecyt 3030065 (Chile). Institutional support to the Centro de Estudios Científicos (CECS) from Empresas CMPC is gratefully acknowledged. CECS is a Millennium Science Institute and is funded in part by grants from Fundación Andes and the Tinker Foundation.

References

- Alexander IJ, Hardy K (1981) Surface phosphatase activity of Sitka spruce mycorrhizas from a serpentine site. *Soil Biol Biochem* 13:301–305
- Alvarez M, Godoy R, Heyser W, Härtel S (2004) Surface bound phosphatase activity in living hyphae of ectomycorrhizal fungi of *Nothofagus obliqua*. *Mycologia* 96:479–487
- Alvarez M, Godoy R, Heyser W, Härtel S (2005) Anatomical–physiological determination of surface bound phosphatase activity in ectomycorrhiza of *Nothofagus obliqua* based on image processed confocal fluorescence microscopy. *Soil Biol Biochem* 37:125–132
- Antibus RK, Kroehler CJ, Linkins AE (1986) The effects of external pH, temperature, and substrate concentration on acid phosphatase activity of ectomycorrhizal fungi. *Can J Bot* 64:2383–2387
- Antibus RK, Sinsabaugh RL, Linkins AE (1992) Phosphatase activities and phosphorus uptake from inositol phosphate by ectomycorrhizal fungi. *Can J Bot* 70:794–801
- Antibus RK, Bower D, Dighton J (1997) Root surface phosphatase activities and uptake of ^{32}P labelled inositol phosphate in field-collected grey birch and red maple roots. *Mycorrhiza* 7:39–46
- Darzynkiewicz Z, Smolewski P, Bedner E (2001) Use of flow and laser scanning cytometry to study mechanisms regulating cell cycle and controlling cell death. *Clin Lab Med* 21:857–873
- de Beer D, Schramm A, Santegoeds CM, Kühl M (1997) A nitrite microsensor for profiling environmental biofilms. *Appl Environ Microb* 63:973–977
- Dexheimer J, Aubert-Dufrense MP, Gérard J, Letacon F, Mousain D (1986) Étude de la localisation ultrastructurale des activités phosphatasiques acides dans deux types d'ectomycorhizes: *Pinus nigra/nigricans*/Hebeloma crustuliniforme et *Pinus pinaster*/Pisolithus tinctorius. *Bull Soc Bot Fr* 133:343–352
- Dickson S, Kolesik P (1999) Visualisation of mycorrhizal fungal structures and quantification of their surface area and volume using laser scanning confocal microscopy. *Mycorrhiza* 9:205–213
- Dighton J (1983) Phosphatase production by mycorrhizal fungi. *Plant Soil* 71:455–462
- Härtel S, Zorn-Kruppa M, Tikhonova S, Heino P, Engelke M, Diehl H (2003) Staurosporine-induced apoptosis in human cornea epithelial cells *in vitro*. *Cytometry* 8:15–23
- Härtel S, Fanani ML, Maggio B (2005a) Shape transitions and lattice structuring of ceramide-enriched domains generated by sphingomyelinase in lipid monolayers. *Biophys J* 88:287–304
- Härtel S, Rojas R, Räth C, Guarda MI, Goicoechea O (2005b) Identification and classification of di- and triploid erythrocytes by multi-parameter image analysis: a new method for the quantification of triploidization rates in rainbow trout (*Oncorhynchus mykiss*). *Arch Med Vet* 37:1–5
- Joner EJ, Johansen A (1999) Phosphatase activity of external hyphae of two arbuscular mycorrhizal fungi. *Mycol Res* 104:81–86
- Kamentsky LA, Kamentsky LD (1991) Microscope-based multi-parameter laser scanning cytometer yielding data comparable to flow cytometry data. *Cytometry* 12:381–387
- Li Y, Dick WA, Tuovinen OH (2004) Fluorescence microscopy for visualization of soil microorganisms—a review. *Biol Fertil Soils* 39:301–311
- McElhinney C, Mitchell DT (1993) Phosphatase activity of four ectomycorrhizal fungi found in a Sitka spruce–Japanese larch plantation in Ireland. *Mycol Res* 97:725–732
- Molina R, Palmer JG (1982) Isolation, maintenance, and pure culture manipulation of ectomycorrhizal fungi. In: Schenck NC (ed) *Methods and principles of mycorrhizal research*. The American Phytopathological Society, St. Paul, pp 115–129
- Nannipieri P, Ceccanti S, Grego S (1990) Ecological significance of the biological activity in soil. In: Bollag JM, Stotzky G (eds) *Soil biochemistry*. Marcel Dekker, New York, pp 293–355
- Smith SE, Read DJ (1997) *Mycorrhizal symbiosis* (2nd ed). Academic Press, London, UK

- Straker CJ, Mitchell DT (1986) The activity and characterisation of acid phosphatases in endomycorrhizal fungi of the Ericaceae. *New Phytol* 104:243–256
- Schweiger PF, Rouhier H, Söderström B (2002) Visualisation of ectomycorrhizal rhizomorph structure using laser scanning confocal microscopy. *Mycol Res* 106:349–354
- Tibbett M, Chambers SM, Cairney JWG (1998) Methods for determining extracellular and surface-bound phosphatase activities in ectomycorrhizal fungi. In: Varma A (ed) *Mycorrhiza manual*. Springer, Berlin Heidelberg New York, pp 217–225
- Tibbett M, Sanders FE, Grantham K, Cairney JW (2000) Some potential inaccuracies of the *p*-nitrophenyl phosphomonoesterase assay in the study of the phosphorus nutrition of soil borne fungi. *Biol Fertil Soils* 31:92–96
- Tibbett M (2002) Considerations on the use of the *p*-nitrophenyl phosphomonoesterase assay in the study of the phosphorus nutrition of soil borne fungi. *Microbiol Res* 157:221–231
- Tisserant B, Gianinazzi-Pearson V, Gianinazzi S, Gollotte A (1993) In planta histochemical staining of fungal alkaline phosphatase activity for analysis of efficient arbuscular mycorrhizal infections. *Mycol Res* 97:245–250
- van Aarle I, Olsson PA, Söderström B (2001) Microscopic detection of phosphatase activity of saprophytic and arbuscular mycorrhizal fungi using a fluorogenic substrate. *Mycologia* 93:17–24
- Wessels JGH (1994) Developmental regulation of fungal cell wall formation. *Annu Rev Phytopathol* 42:413–437